Proceedings of the 28th IEEE
EMBS Annual International Conference
New York City, USA, Aug 30-Sept 3, 2006

Multi-modal Medical Image Registration Based on Adaptive Combination of Intensity and Gradient Field Mutual Information

Jiangang Liu, Jie Tian* *Senior Member, IEEE* and Yakang Dai

Abstract— **Mutual information (MI) is an effective criterion for multi-modal image registration. However the traditional MI function only includes intensity information of images and lacks sufficient spacial information to accurately measure the degree of alignment of two images, and besides, it is apt to be influenced by intensity interpolation, therefore presents many local maxima which frequently lead to misregistration. Our paper proposes a criterion of adaptive combination of intensity and gradient field mutual information (ACMI). Unlike the intensity MI computed from two original images, the gradient field MI of two images is calculated from their gradient code maps (GCM) constructed by coding the gradient field information of corresponding original image. Because of their complementary properties, these two MI functions are combined to form ACMI by a nonlinear weight function which can be adaptively regulated according to their performances and make the better dominant in the combination. Experimental results demonstrate that the ACMI outperforms the traditional MI and furthermore the former is much less sensitive than the latter to the reduction of resolution or overlapped region of images.**

I. INTRODUCTION

Multi-modal image registration plays a significant role in medical image processing. Mutual information (MI) is an effective criterion for the multi-modal medical image registration [1], [2]. However, even with this method, the correct alignment is not guaranteed, especially when it is applied to images with low resolution or small overlapped region, because the traditional MI function only includes intensity information of images and lacks sufficient spacial information to accurately measure the degree of alignment of two images, and besides, it is apt to be influenced by intensity interpolation, therefore presents many local maxima which frequently lead to misregistration [3], [4].

Different tissue in human brain presents different gray intensity no matter which imaging modality is applied to them. So the intensity gradient at the transition of two tissues is steeper than the interior, where the magnitude and phase of the gradient mostly lie on the imaging modality, but its spatial relative position is basically invariable. So the gradient fields of two images can provide reliable spatial information for their similarity measurement. Some researches introduced gradient information into image registration to improve its quality [5], [6], [7]. Though these methods proved to be effective, they neither took full advantage of the phase information of gradient field nor took account of the relationship between intensity images and their gradient fields. Our work follows this direction and integrates both magnitude and phase information of gradient field into traditional MI in a flexible way to further improve the performance of MI function.

In current study, we propose a multi-modal image registration technique, namely adaptive combination of intensity and gradient field mutual information (ACMI). Unlike the intensity MI computed directly from two original images, the gradient field MI is calculated from the gradient code maps (GCM) obtained from corresponding original images by a spherical gradient coder. The intensity of each point in GCM is completely determined by the gradient vector of corresponding point in original image, so that the magnitude and phase information of gradient field of original image is converted into intensity information of GCM. The properties of these two MI functions are complimentary for each other. The ACMI is defined as the sum of productions of each MI function and its respective weight which can be adaptively regulated to highlight the MI function with better performance.

The results of simulated data show that ACMI function is much smoother and more reliable than traditional MI. And the statistical test for the results of actual registration demonstrates that the registration quality with ACMI is significantly higher than that with traditional MI, and besides the former is much less sensitive than the latter to the reduction of resolution or overlapped region of images.

II. METHOD

A. Mutual information

Given image R and F with respective entropy $H(R)$ and $H(F)$ and their joint entropy $H(R,F)$, their MI $I(R,F)$ and entropy correlation coefficient (ECC) $E(R,F)$ [8], another registration criterion, are defined respectively as

$$I(R,F) = H(R) + H(F) - H(R,F), \qquad (1\text{-}1)$$

$$E(R,F) = \frac{2I(R,F)}{H(R)+H(F)}. \qquad (1\text{-}2)$$

For fixed images R and F, their respective entropies $H(R)$ and $H(F)$ are both approximately constant, so the value of EEC can be regarded as the production of $I(R,F)$ and a constant. Accordingly, ECC has similar performance to MI except its normalized value range ([0, 1]). Then, in following analyse, ECC will be used in place of corresponding MI.

This work is supported by NSFDYS(60225008), NSFC(30370418, 90209008, 60302016, 60532050 and 30500131), JRFOCYS(30528027) and BNSF(4051002 and 4042024) in China.

J. Liu, J. Tian and Y. Dai are with Medical Image Processing Group, Key Laboratory of Complex Systems and Intelligence Science, Institute of Automation Chinese Academy of Science. Email: tian@ieee.org

B. Spatial gradient coder

Given a 2D image F with intensity $f(x,y)$, its spatial gradient field $G_F(x,y)$ can be computed by

$$G_F(x,y) = \frac{\partial f(x,y)}{\partial x}\overrightarrow{i} + \frac{\partial f(x,y)}{\partial y}\overrightarrow{j},$$

where the $\overrightarrow{i}$ and $\overrightarrow{j}$ are the unit vector along x and y axis, respectively. If the horizontal and vertical derivatives, namely $\frac{\partial f(x,y)}{\partial x}$ and $\frac{\partial f(x,y)}{\partial y}$, are denoted by f_x and f_y, respectively, then the magnitude $\rho_{i,j}$ and phase $\theta_{i,j}$ ($[-\pi,\pi)$) of gradient of voxel $f_{i,j}$ are calculated by

$$\rho_{i,j} = \sqrt{f_x^2 + f_y^2}$$
$$\theta_{i,j} = \begin{cases} \tan^{-1}(f_y/f_x) & f_x > 0 \\ \tan^{-1}(f_y/f_x) + \pi & f_x < 0, f_y > 0 \\ \tan^{-1}(f_y/f_x) - \pi & f_x < 0, f_y < 0 \\ \pi/2 & f_x = 0, f_y > 0 \\ -\pi/2 & f_x = 0, f_y < 0. \end{cases} \quad (2)$$

For convenience, the $\rho_{i,j}$ is normalized into range [0,1]. Then the point $c_{i,j}$ in GCM C is obtained by coding the gradient vector ($\rho_{i,j}$, $\theta_{i,j}$) of corresponding point $f_{i,j}$ in F with gradient coder [7]

$$c_{i,j} = \begin{cases} \lfloor \frac{\rho_{i,j}}{\Delta_\rho} \rfloor N + \lfloor \frac{\theta_{i,j}}{\Delta_\theta} \rfloor & \text{if } \rho_{i,j} \geq Th \\ 0 & \text{if } \rho_{i,j} < Th, \end{cases} \quad (3)$$

where $\lfloor x \rfloor$ is the integer partion of x and Th is a pre-specified threshold to ignore the point with low gradient magnitude. N equals to $2\pi/\Delta_\theta$, and Δ_ρ and Δ_θ are respectively the magnitude and phase bin-intervals of gradient coder. The GCM includes both magnitude and phase information, so it provides more spacial information for measurement of similarity of two images. Fig. 1 illustrates a 2D gradient coder.

This gradient coder can be easily extended to 3D images. Given a voxel $f_{i,j,k}$ of 3D image F with gradient vector (f_x, f_y, f_z), the 3D gradient coder is defined as:

$$c_{i,j,k} = \begin{cases} \lfloor \frac{\rho_{i,j,k}}{\Delta_\rho} \rfloor NK + \lfloor \frac{\phi_{i,j,k}}{\Delta_\phi} \rfloor K + \lfloor \frac{\theta_{i,j,k}}{\Delta_\theta} \rfloor & \text{if } \rho_{i,j,k} \geq Th \\ 0 & \text{if } \rho_{i,j,k} < Th \end{cases} \quad (4)$$

with

$$\rho_{i,j,k} = \sqrt{f_x^2 + f_y^2 + f_z^2}$$
$$\phi_{i,j,k} = \cos^{-1}(f_z/\rho_{i,j,k}),$$

where $\phi_{i,j,k}$ ($[0,\pi]$) and $\theta_{i,j,k}$ ($[-\pi,\pi)$) are the polar angle and azimuthal angle, respectively, and $\theta_{i,j,k}$ is calculated similarly to $\theta_{i,j}$ in (2). N and K equal to π/Δ_ϕ and $2\pi/\Delta_\theta$, respectively where Δ_ϕ and Δ_θ are the polar angle and azimuthal angle bin-intervals of 3D gradient coder, respectively. The other notations are defined similarly as in (3). Thus, with (4), spatial gradient information of original images is converted into intensity information of GCMs. Fig. 2 and Fig. 3 show a slice of a 3D MRI T1 and 3D PET GCM, respectively.

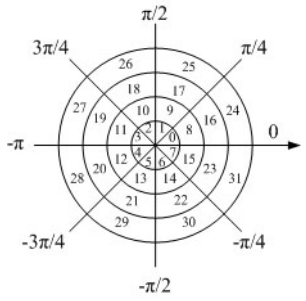

Fig. 1. Illustration of a 2D gradient coder ($\Delta_\rho = 1/4$, $\Delta_\theta = \pi/4$).

C. Adaptive Combination of intensity and gradient field MI (ACMI)

With (1), the intensity ECC E_i and the gradient field ECC E_g are obtained from two original images and their GCMs, respectively. The ACMI E_a is defined as:

$$E_a = f(v(E_i,E_g))E_i + (1 - f(v(E_i,E_g)))E_g \quad (5)$$

with

$$f(v(E_i,E_g)) = \frac{1}{1 + exp(-(v(E_i,E_g) - 0.5)/T)}$$
$$v(E_i,E_g) = \frac{E_i + E_g}{2} \qquad 0 \leq E_i, E_g \leq 1.$$

As shown in Fig. 4, the weighting function $f(v(E_i,E_g))$ actually is a logistic function with rightward half unit shift, where T is an "time constant" controlling the shape of weighting function. This function has some expected properties [9]. The first is saturation with the maximum of one and minimum of zero, just corresponding to the value range of weights used in ACMI. The second is differentiability which not only prevents additional local maxima being introduced by combination of registration functions but also facilitates the optimization of ACMI with some derivative-needed techniques such as Gauss-Newton method. The third, the most important, is the nonlinearity. As shown in Fig. 4, the weighting function presents nonlinear characteristic in two terminal saturating parts but approximately presents linear characteristic in the middle non-saturating part. Thus, according to (5), the ACMI is mostly determined by one of two ECC functions at two terminals (gradient field ECC for the left terminal and intensity ECC for the right), but equals the sum of two ECC functions with similar weights in the middle part. This weight-similar sum probably leads to severe roughness of ACMI. So the weighting function should shorten its unexpected middle linear part and lengthen the terminal saturating parts. But extremely nonlinearity can make middle part of weighting function exceedingly steep, and therefore destroy the differentiability of ACMI function. By experience, 0.04 is a practical choice for T. In term of these properties, $f(v(E_i,E_g))$ is a desirable weighting function for combination of registration functions.

As shown in Fig. 2 (a) and Fig. 3 (a), the original images contain abundant information. This has two effects on their

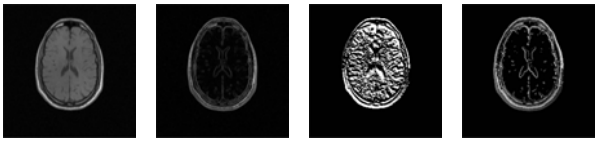

(a) (b) (c) (d)

Fig. 2. A slice of 3D GCM of MRI T1. (a) original image, (b) gradient magnitude map, (c) gradient phase map, (d) GCM ($\Delta_\rho = 1/16$, $\Delta_\theta = \pi/8$, $\Delta_\phi = \pi/8$ and Th=0.10).

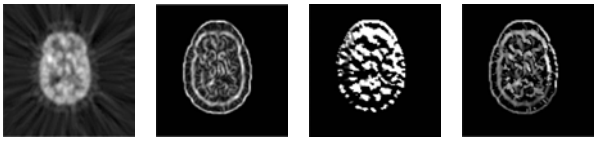

(a) (b) (c) (d)

Fig. 3. A slice of 3D GCM of PET. (a) original image, (b) gradient magnitude map, (c) gradient phase map, (d) GCM ($\Delta_\rho = 1/16$, $\Delta_\phi = \pi/8$, $\Delta_\theta = \pi/8$ and Th=0.16.)

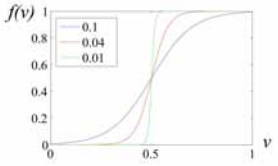

Fig. 4. Weighting function $f(v(E_i, E_g))$ with T=0.01 (green), T=0.04 (red) and T=0.1 (blue), respectively.

ECC function. One hand, the abundant information makes the similarity measure of two images more reliable, i. e. the global maximum corresponds to the correct alignment approximately, so the ECC function presents a tendency of convergence to this global maximum. On the other hand, abundant information means strong non-uniformity of intensity across voxels, then the ECC function is easily influenced by intensity interpolation, and thereby presents many local maxima leading to misregistration [3].

Compared to their original images, as shown in Fig. 2 (d) and Fig. 3 (d), GCMs contain less information (most voxels have zero intensity value except ones at edges of some tissues). This comparatively higher intensity uniformity reduces the effect of intensity interpolation on ECC function of two maps and therefore makes it smoother [3]. Additionally the edge information in GCMs can provide reliable and accurate spatial information for the similarity measure of images. However, in the neighborhood of global maximum, this ECC function often presents plateaus or valleys making its convergence to global maximum difficult.

According to their complementary properties, these two ECC functions are combined as a new registration function (ACMI) by (5) with a weighting function whose value varies with the sum of two ECC values. Thus at the coarse registration stage, the ACMI depends mostly on gradient field ECC due to low sum of ECC values and presents a smooth property facilitating the convergence to the basin of global maximum. At the fine stage, the ACMI is determined mostly by intensity ECC for which the gradient field ECC is a supplement. The higher the sum of ECCs is, the more reliable the intensity ECC is, therefore the more the ACMI depends on it than on gradient field ECC. This coarse-to-fine and gradient-to-intensity strategy guarantees the convergence to global maximum corresponding to correct alignment.

III. Result

The brain image pairs (MRI T1, PD, T2 and their rectified versions vs. PET) are provided by Vanderbilt University [10]. To evaluate the performances of traditional ECC and ACMI for image pairs with low resolution or small overlapped area, two types of image pairs are generated from each original image pair , namely sub-sampled version (subsampled by a factor of two in three axes respectively) and small-overlapped version (50% overlapped region of original pairs). For the following experiments, by experience, the Δ_ρ, Δ_ϕ and Δ_θ of gradient coder are $1/16$, $\pi/8$ and $\pi/8$, respectively, and the threshold Th for each type image is: 0.10 for MRI T1, 0.08 for MRI T2, 0.12 for MRI PD and 0.16 for PET.

Fig. 5 describes three types of registration functions of a PET/MRI T1 pair, namely intensity ECC (traditional ECC), gradient field ECC and their adaptive combination ACMI vs. displacements in horizontal and vertical orientation. For each image version, ACMI function is smoother and more reliable than intensity MI. For the sub-sampled version, the intensity ECC function presents many local maxima and two global maxima; the gradient field ECC function presents less local maxima but a narrow valley at the bottom hindering the optimization from reaching the global maximum. For the small-overlapped version, the intensity ECC function also has multiple local maxima and one global maximum corresponding to the correct alignment approximately; the gradient field ECC is comparatively smoother but presents a plateau at the bottom not including the point corresponding to the correct alignment. So even the global optimization method such as Simulated Annealing is applied to these versions, the correct alignment is not guaranteed.

For each image pair, the registrations are applied to its three type versions with traditional ECC and ACMI, respectively. Partial volume interpolation and simplex downhill optimization methods are employed in these registrations. The accuracy of each registration is evaluated by "Retrospective Image Registration Evaluation" project using bone-marker-based gold standard (See [10] for more detail). Table I summarizes the results of registrations, and the values therein are the errors of distances between the gold standard and the centroids of volume of interest (VOIs) transformed from floating image by our methods.

For each of three image versions(original version, sub-sampled version and small-overlapped version), a paired student t test on ECC types reveals that the results of ACMI are significantly more accurate than those of traditional ECC (p <0.01 for original version, p <0.0001 for sub-sampled version and small-overlapped version). For each of ECC type (ACMI/traditional ECC), The one-way analysis of

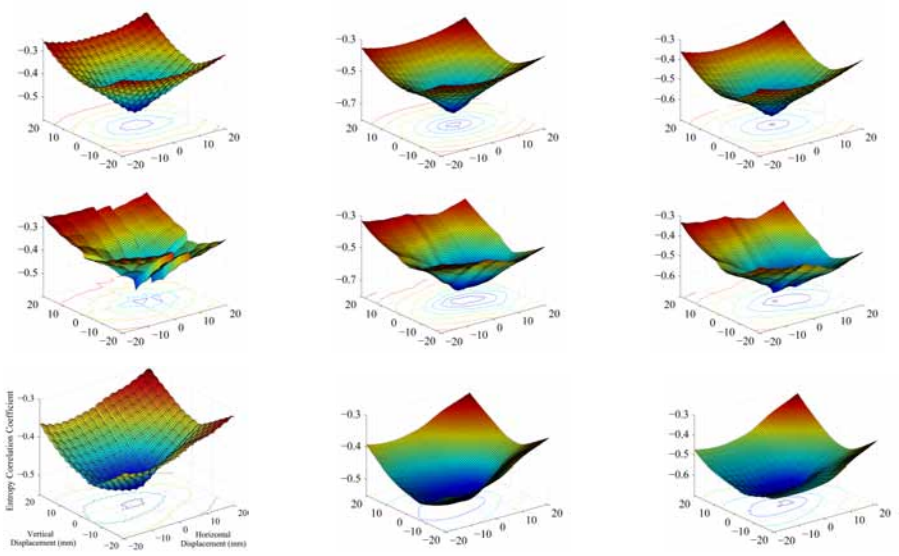

(a) (b) (c)

Fig. 5. Registration function (PET/MRI T1) vs. displacement in horizontal and vertical axes. Column (a): intensity ECC; column (b): gradient field ECC; Column (c): ACMI. From top to bottom: registration functions of (i) original images; (ii) sub-sampled version; (iii) small-overlapped version.

TABLE I
ACCURACY COMPARISON OF TRADITIONAL ECC VS. ACMI (TRADITIONAL ECC/ACMI)(MM).

	PET-MRI(Rectified)		PET-MRI	
	Median	Maximum	Median	Maximum
Original images				
T1	2.78/2.38	4.96/4.22	3.19/2.63	8.37/5.43
T2	1.91/1.39	6.37/5.51	3.15/2.72	9.15/6.08
PD	2.46/1.62	6.19/3.41	3.07/2.37	8.13/6.74
Sub-sampled version				
T1	4.13/3.40	8.25/7.48	4.62/3.51	10.37/8.83
T2	4.14/3.06	9.18/5.10	5.25/4.83	16.15/7.07
PD	3.07/2.59	12.94/5.36	4.17/3.03	11.82/6.33
Small-overlapped version				
T1	4.15/3.33	5.78/7.17	3.33/2.61	10.85/6.72
T2	3.34/2.20	8.37/4.94	4.17/3.21	12.05/7.38
PD	3.98/2.84	8.18/5.11	3.16/3.39	9.10/6.91

For each column, the left numbers of solidus (/) correspond to the traditional ECC and the right to the ACMI.

variance (ANOVA) on three image versions finds significant difference for traditional ECC (p <0.001), but not for ACMI (p >0.05). This reveals that ACMI function is much less sensitive to the reduction of resolution or overlapped area of images than the traditional ECC. In addition, sub-pixel accuracy is obtained in all registrations with ACMI.

IV. DISCUSSION AND CONCLUSION

We have proposed a technique for multi-modal image registration based on adaptive combination of intensity and gradient field mutual information, i.e. ACMI, which combines the advantages of these two MI function and overcomes the roughness and unreliability of the traditional MI function. Results of simulated data experiments and the actual registration both demonstrate that ACMI function not only has better performance but also presents less sensitivity to the reduction of resolution or overlapped area of two images compared with the tradition MI. So ACMI function is suitable for the registration of low-resolution images or impaired images. We will apply this method to non-rigid registration in near future.

ACKNOWLEDGMENTS

The images and the standard transformation(s) were provided as part of the project, "Retrospective Image Registration Evaluation", Vanderbilt University, Nashville, TN.

REFERENCES

[1] P. Viola and W. M. Wells III. Alignment by maximization of mutual information. In *Proc. 5th Int. Conf. Computer Vision*, pages 16–23, Cambridge, MA, 1995.

[2] F. Maes, A. Collignon, D Vandermeulen, G. Marchal, and Paul Suetens. Multimodality image registration by maximization of mutual information. *IEEE Trans. Med. Imag.*, 16(2):187–198, 1997.

[3] J. P. W. Pluim, J. B. A. Maintz, and M. A. Viergever. Interpolation artefacts in mutual information-based image registration. *Computer Vision and Image Understanding*, 77(2):211–232, 2000.

[4] Jeffrey Tsao. Interpolation artifacts in multimodality image registration based on maximization of mutual information. *IEEE Trans. Med. Imag.*, 22(7):235–260, 2003.

[5] J. P. W. Pluim, J. B. A. Maintz, and M. A. Viergever. Image registration by maximization of combined mutual information and gradient information. *IEEE Trans. Med. Imag.*, 19:809–814, 2000.

[6] E. Haber and J. Modersitzki. Intensity gradient based registration and fusion of multi-modal images. Technical Report TR-2004-027-A, Department of Mathematics and Computer Science, Emory University, Atlanta GA 30322, Jun 2004.

[7] Xiaoxiang Wang and Jie Tian. Image registration based on maximization of gradient code mutual information. *Image Anal Stereol*, 24:1–7, 2005.

[8] F. Maes. *Segmentation and registration of multimodal medical images: From theoty, implementation and validation to a useful tool in clinical practice*. Ph.D., Catholic University of Leuven, Leuven, Belgium, 1998.

[9] P. E. Hart R. O. Duda and D. G. Stork. *Pattern Classification Second Edition*. China Machine Press, Beijing, 2004.

[10] J. West and J. M. Fitzpatrick et al. Comparison and evaluation of retrospective intermodality brain image registration techniques. *Journal of Computer Assisted Tomography*, 21(4):554–566, 1997.